Electronic Supplementary Material (ESI) for New Journal of Chemistry.

Dual-colored 4,4',4'',4'''-(cyclobutane-1,2,3,4-tetrayl)-tetrabenzoate electrochromic materials with large optical contrast and coloration efficiency

Chun-rong Zhu, Jia-ping Xie, Hong-rong Mou, Zhen-jie Huang, Qian-Tang,* Cheng-Bin Gong,* Xiang-Kai Fu

The Key Laboratory of Applied Chemistry of Chongqing Municipality, Chongqing Key Laboratory of Soft-Matter Material Chemistry and Function Manufacturing, College of Chemistry and Chemical Engineering, Southwest University, Chongqing, 400715, China.

S1 Solubility behavior of CBTBAs

Table S1 Solubility behavior of CBTBAs

Compound	Chloroform	CH_2Cl_2	NMP	DMF	THF	Ethyl acetate	Butyl acetate	Toluene
a	++	++	++	++	++	++	++	—
b	++	++	++	++	++	++	++	—
c	++	++	++	++	++	++	++	—
d	++	++	++	++	++	++	++	—
e	++	++	++	++	++	—	—	—
f	++	++	++	++	++	—	—	—
g	++	++	++	++	++	—	—	—
h	++	++	++	++	++	+—	+—	—
i	+—	+—	++	++	++	—	—	—

The solubility was determined with a 50 mg sample in 1 mL solvent. ++ denotes soluble at room temperature; +— denotes partially soluble or swelling; — denotes insoluble even on heating.

S2 NMR and mass spectra

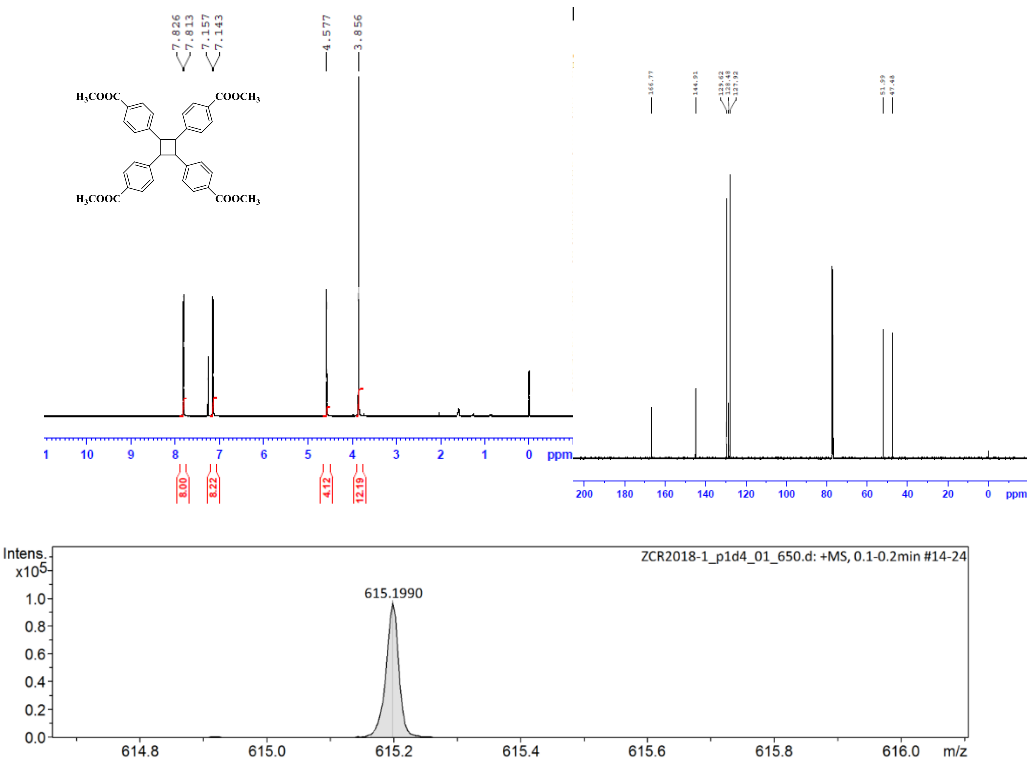

Fig. S1 ^{1}H NMR (top, left), ^{13}C NMR (top, right), and mass spectra (bottom) of compound **a**.

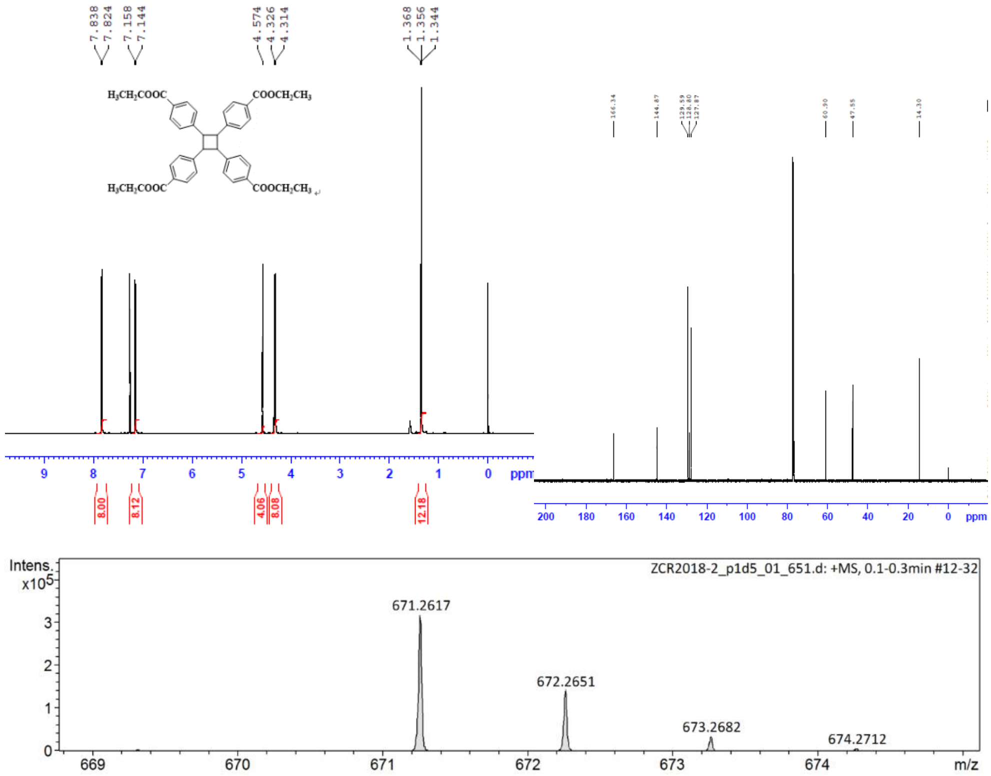

Fig. S2 [1]H NMR (top, left), [13]C NMR (top, right), and mass spectra (bottom) of compound **b**.

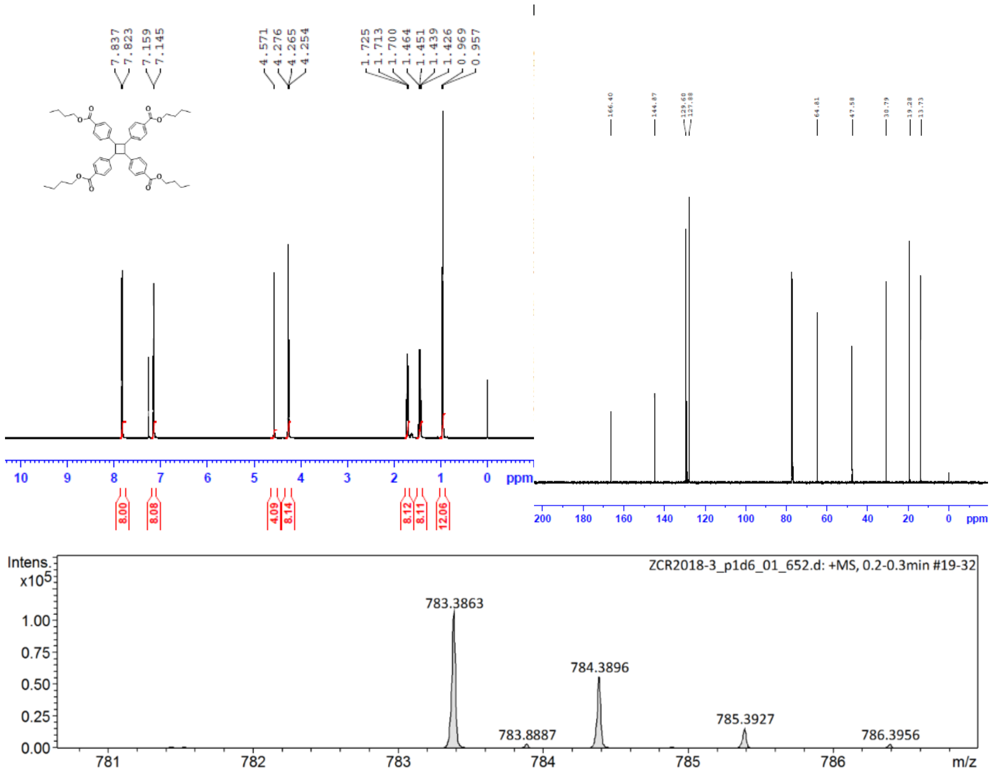

Fig. S3 [1]H NMR (top, left), [13]C NMR (top, right), and mass spectra (bottom) of compound **c**.

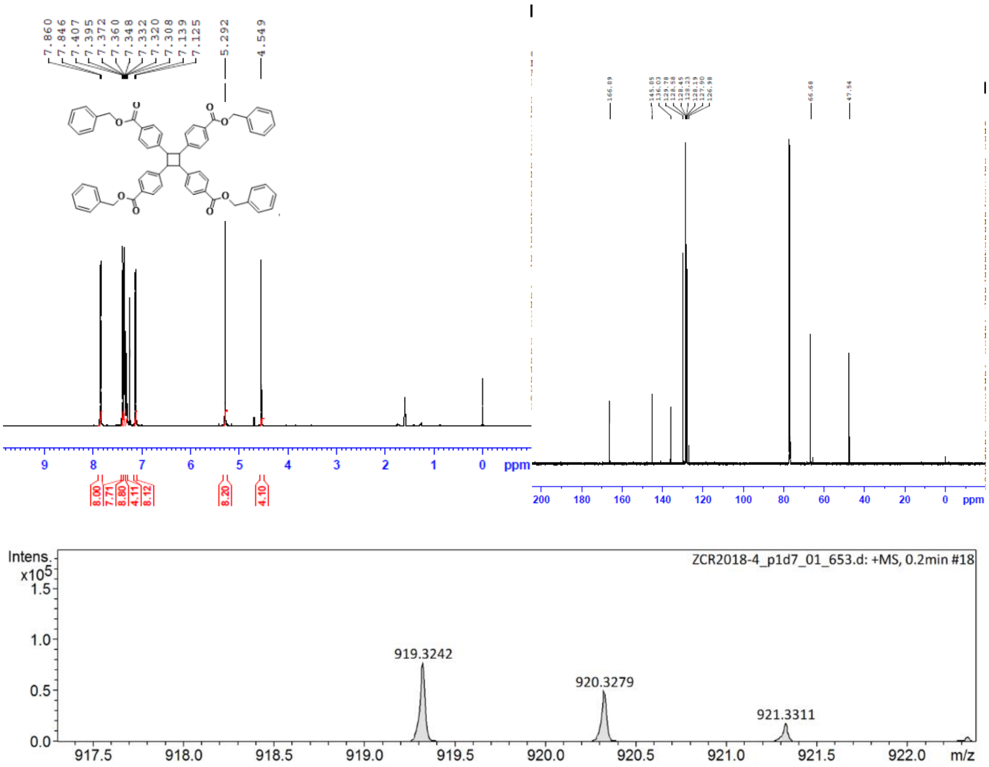

Fig. S4 ^{1}H NMR (top, left), ^{13}C NMR (top, right), and mass spectra (bottom) of compound **d**.

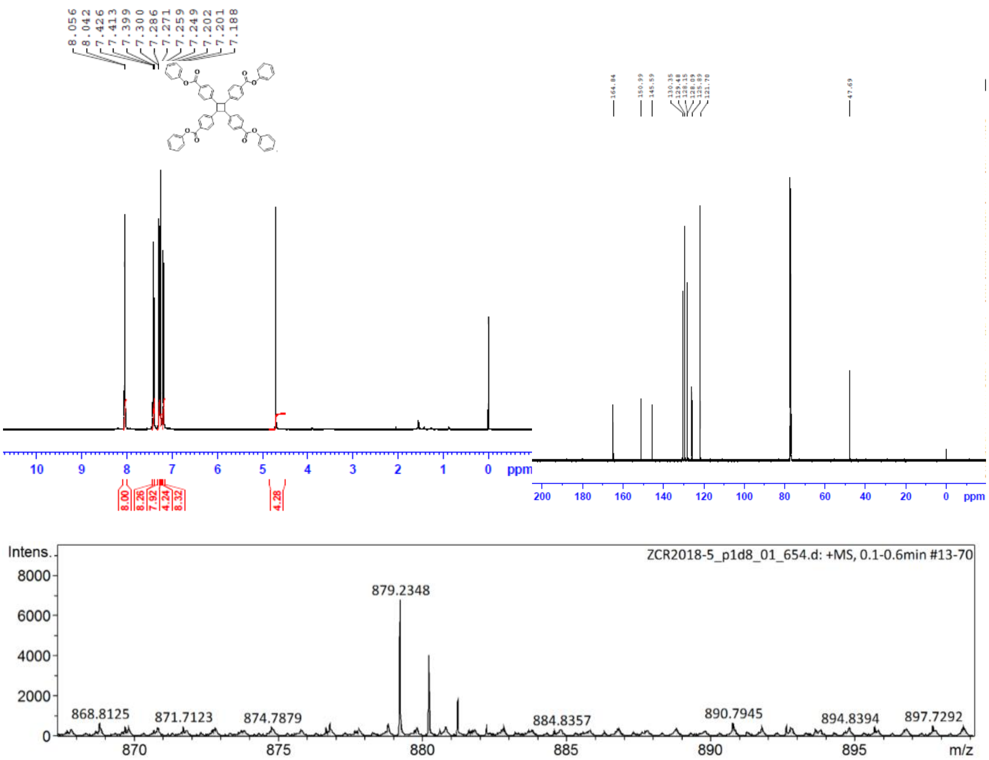

Fig. S5 ^{1}H NMR (top, left), ^{13}C NMR (top, right), and mass spectra (bottom) of compound **e**.

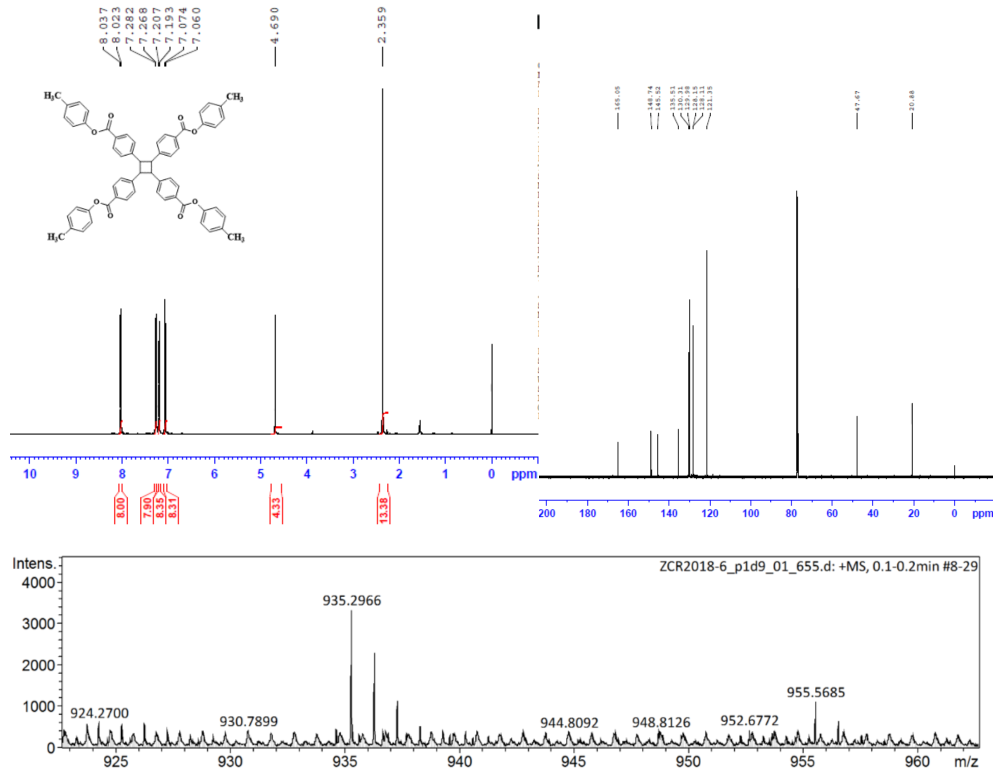

Fig. S6 ^{1}H NMR (top, left), ^{13}C NMR (top, right), and mass spectra (bottom) of compound **f**.

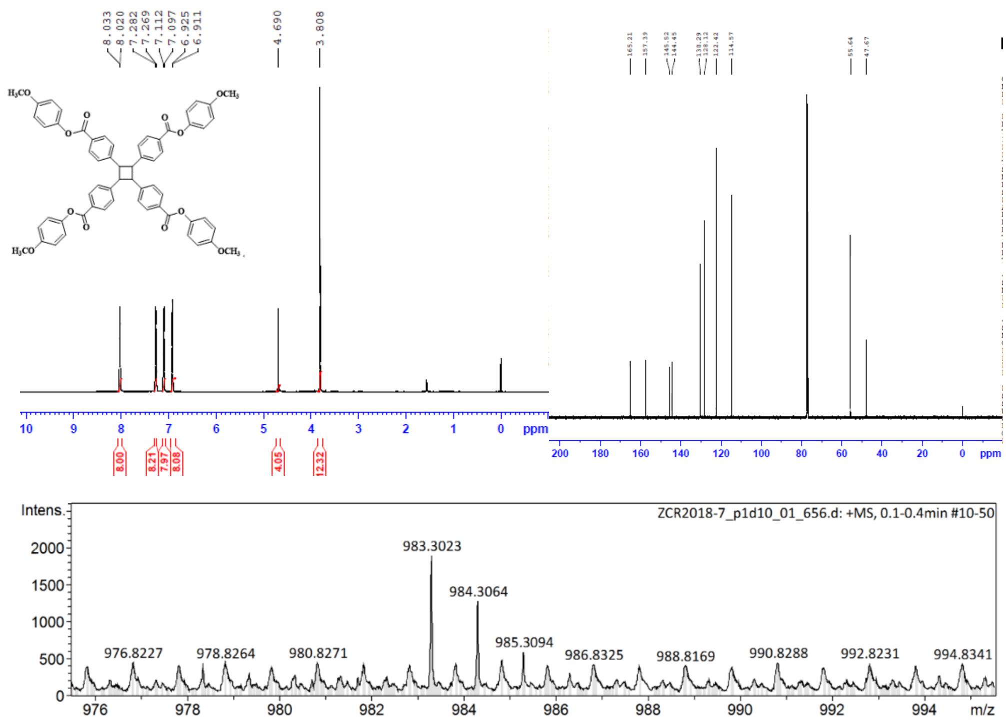

Fig. S7 ^{1}H NMR (top, left), ^{13}C NMR (top, right), and mass spectra (bottom) of compound **g**.

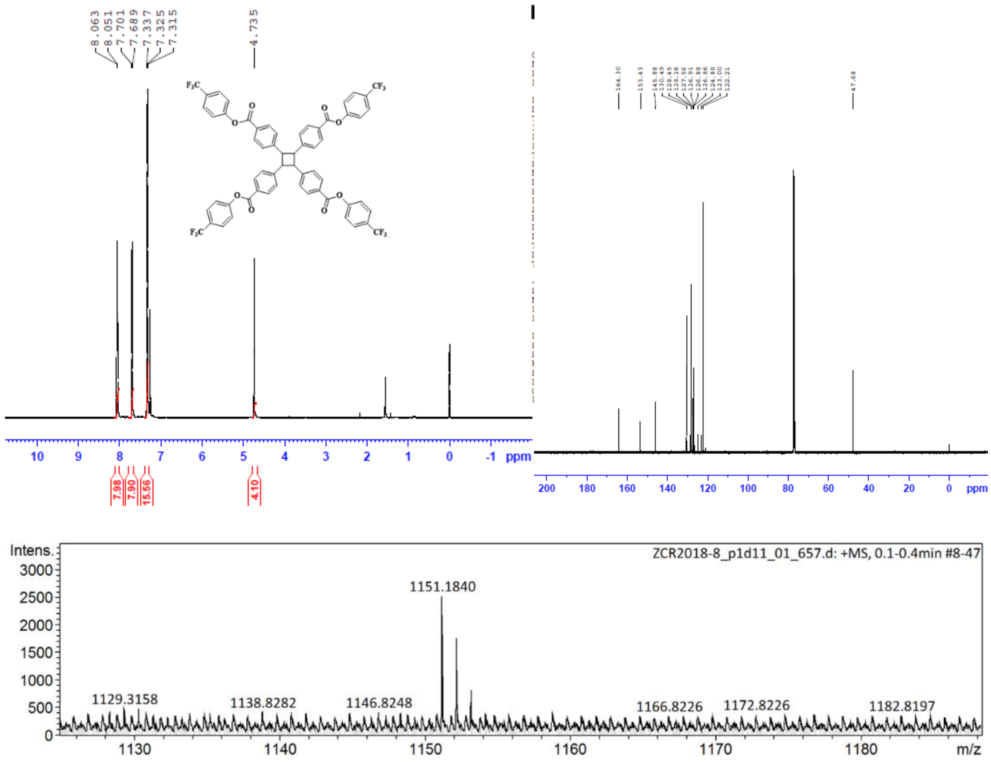

Fig. S8 ^{1}H NMR (top, left), ^{13}C NMR (top, right), and mass spectra (bottom) of compound **h**.

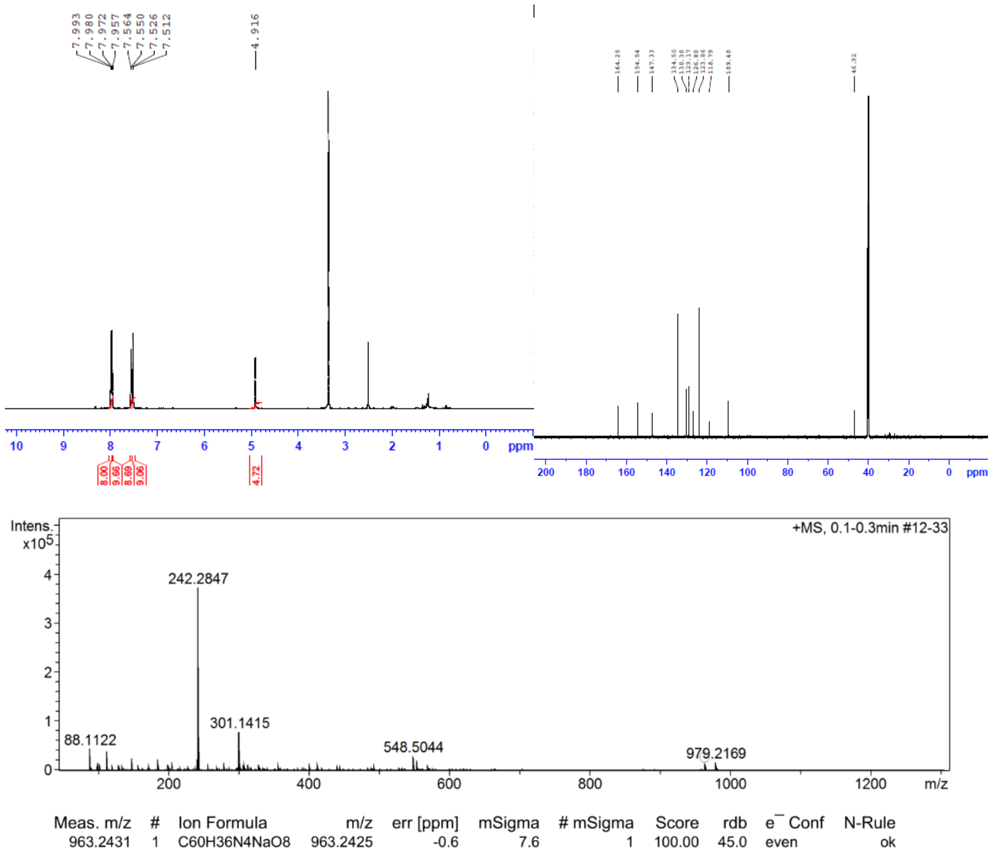

Fig. S9 ^{1}H NMR (top, left), ^{13}C NMR (top, right), and mass spectra (bottom) of compound **i**.

S3 ECD construction

The schematic diagram of the ECD is shown in Scheme S1.Ferrocene (Fc) was used as a counter redox material to stabilize ECD. The reactions of color change in the device are mainly as follows:

$$Fc - 2e^{-} = Fc^{2+}; \quad (1)$$

$$CATBAs^{-} + e^{-} = CATBAs^{2-}; \quad (2)$$

$$CATBAs^{2-} + e^{-} = CATBAs^{3-}; \quad (3)$$

Fc loses electrons in the device to undergo an oxidation reaction, and the EC material undergoes an electron reduction reaction while also undergoing a color change. The role of Fc is to provide electrons for the reduction of EC materials to make the reaction faster, thereby accelerating the response time of the device and appropriately reducing the driving voltage.

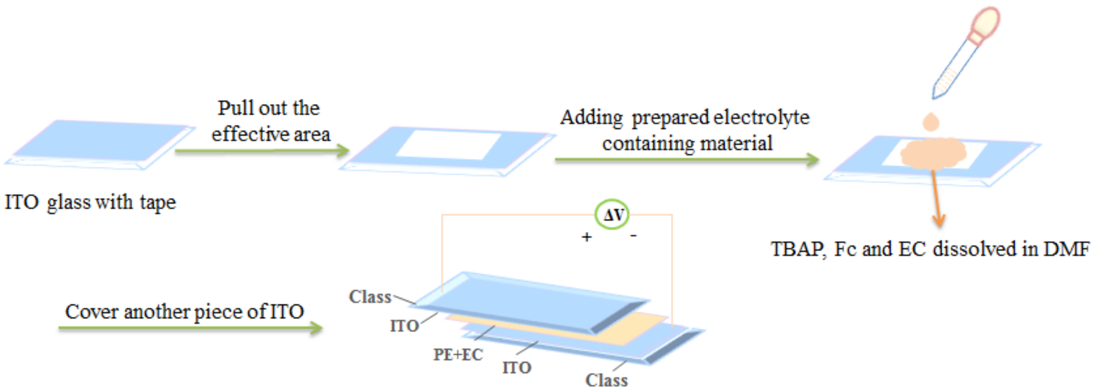

Scheme S1 ECD structure diagram

S4 Crystal data and structure refinement

Table S2 Crystal data and experimental parameters for compound **b**

Compound	**b**
Formula	$C_{40}H_{40}O_8$
Fw	648.27
Crystal system	triclinic
Space group	P-1
a/Å	7.7762(2)
b/Å	8.2847(4)
c/Å	13.7706(6)
α/°	99.715(4)
β/°	94.914(3)
γ/°	94.610(3)
Volume/Å^3	867.14(6)
Z	1
ρ_{calc} /g/cm^3	1.242
μ/mm^{-1}	0.698
radiation	CuKα
size (mm)	0.20 × 0.20 × 0.20
F(000)	344.0
2θ range (deg)	10.886 to 146.06
reflns collected	9530
indep. reflns	3389 (R_{int} = 0.0223)
reflns obs. [$I > 2\sigma(I)$]	3008
data/restr/paras	3389/ 37/ 239
GOF	1.048
R1/wR2 [$I >= 2\sigma(I)$]	0.0580 / 0.1631
R1/wR2 (all data)	0.0621 / 0.1684
largest diff. peak/hole / e Å^{-3}	0.20 / -0.23
CCDC	1936928

S5 Molecular orbital diagrams of CBTBAs

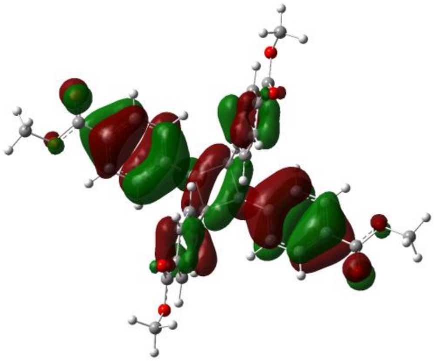

HOMO-a

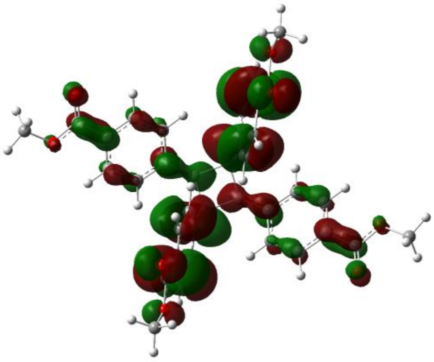

LUMO-**a**

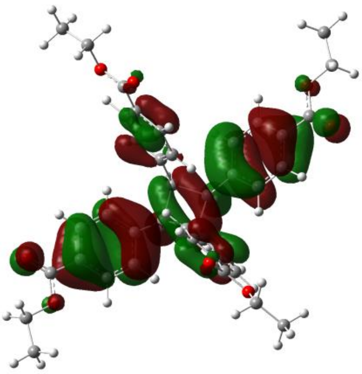

HOMO-**b**

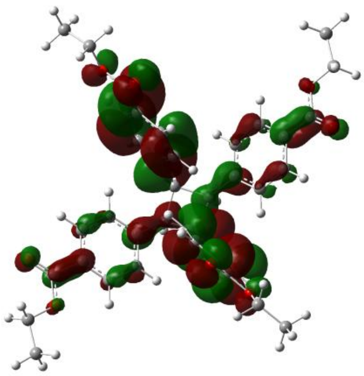

LUMO-**b**

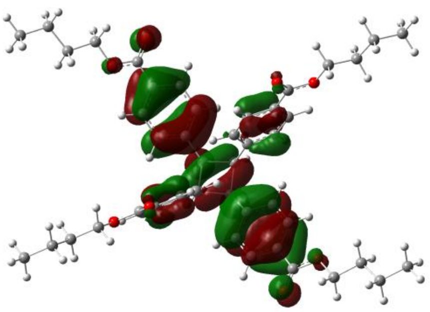

HOMO-**c**

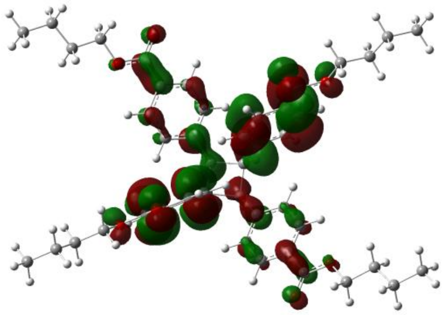

LUMO-**c**

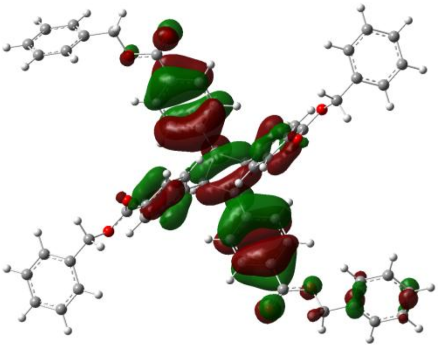

HOMO-**d**

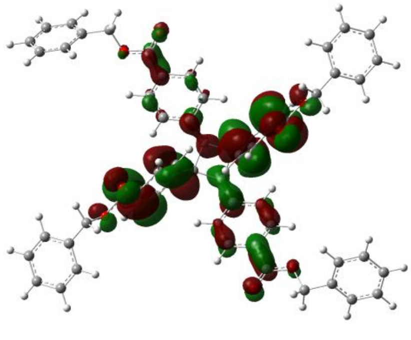

LUMO-**d**

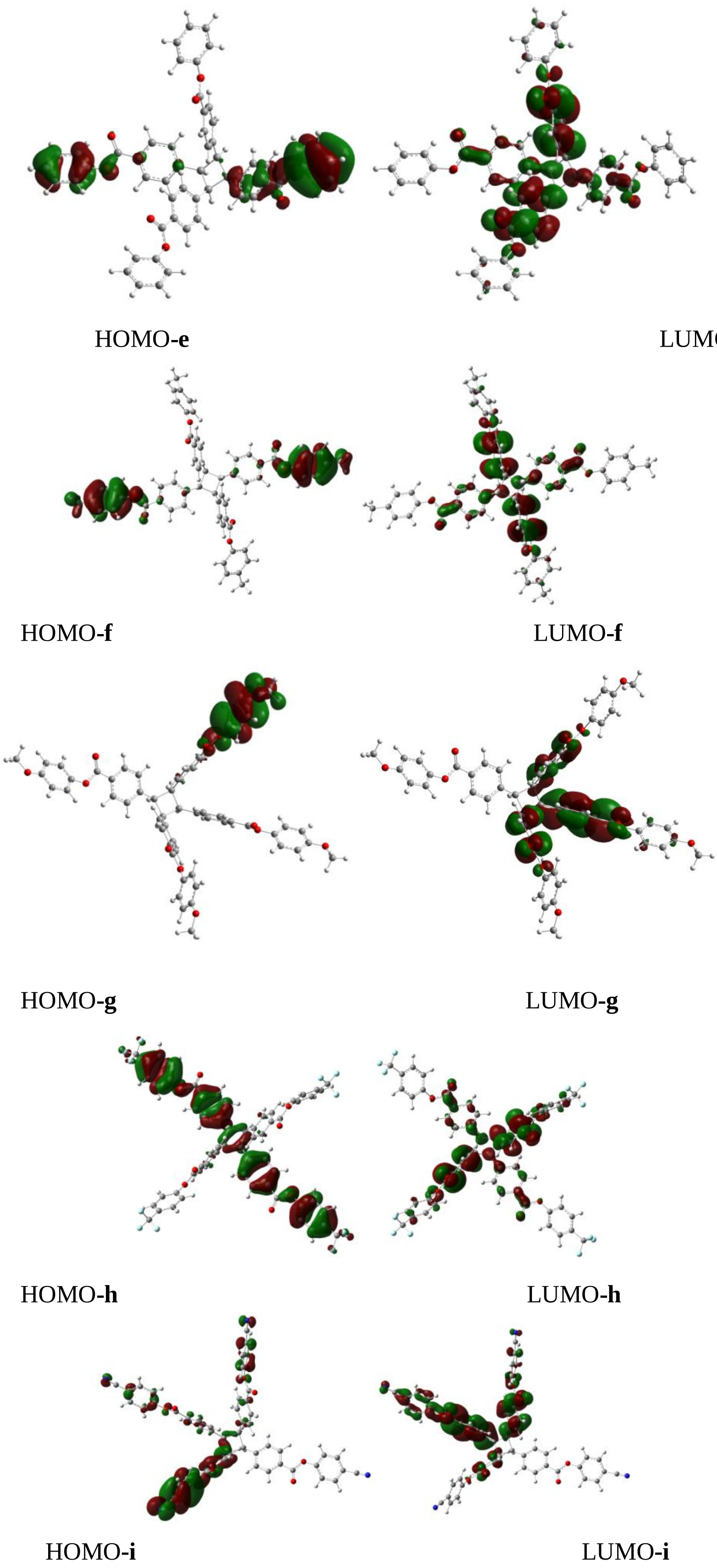

Fig. S10 The molecular orbital diagram of CBTBAs.

S6 Cyclic voltammograms

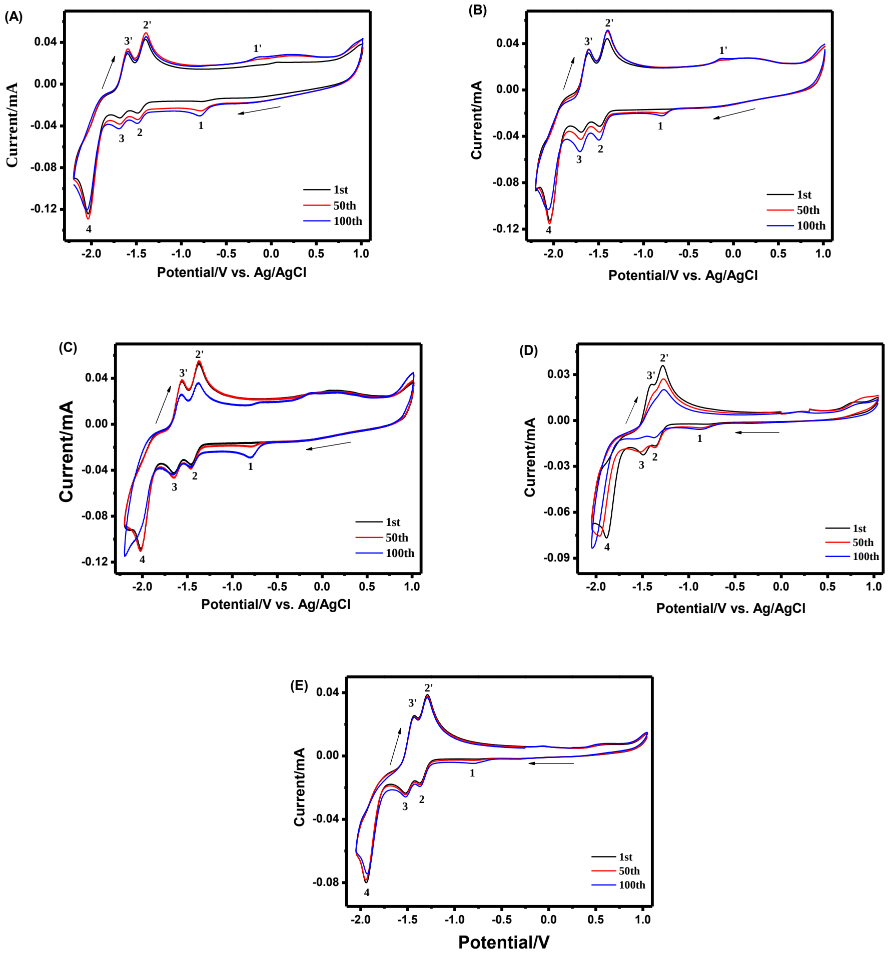

Fig. S11 Cyclic voltammograms of 1 mmol L^{-1}compounds **a** (A), **c** (B), **d** (C), **e** (D), and **g** (E) cycled 100 times between −2.20 and 1.05 V vs. Ag/AgCl of in 50 mmol L^{-1} $TBAPF_6$/DMF at 100 mV s^{-1}.

S7 UV-Vis Spectroscopy

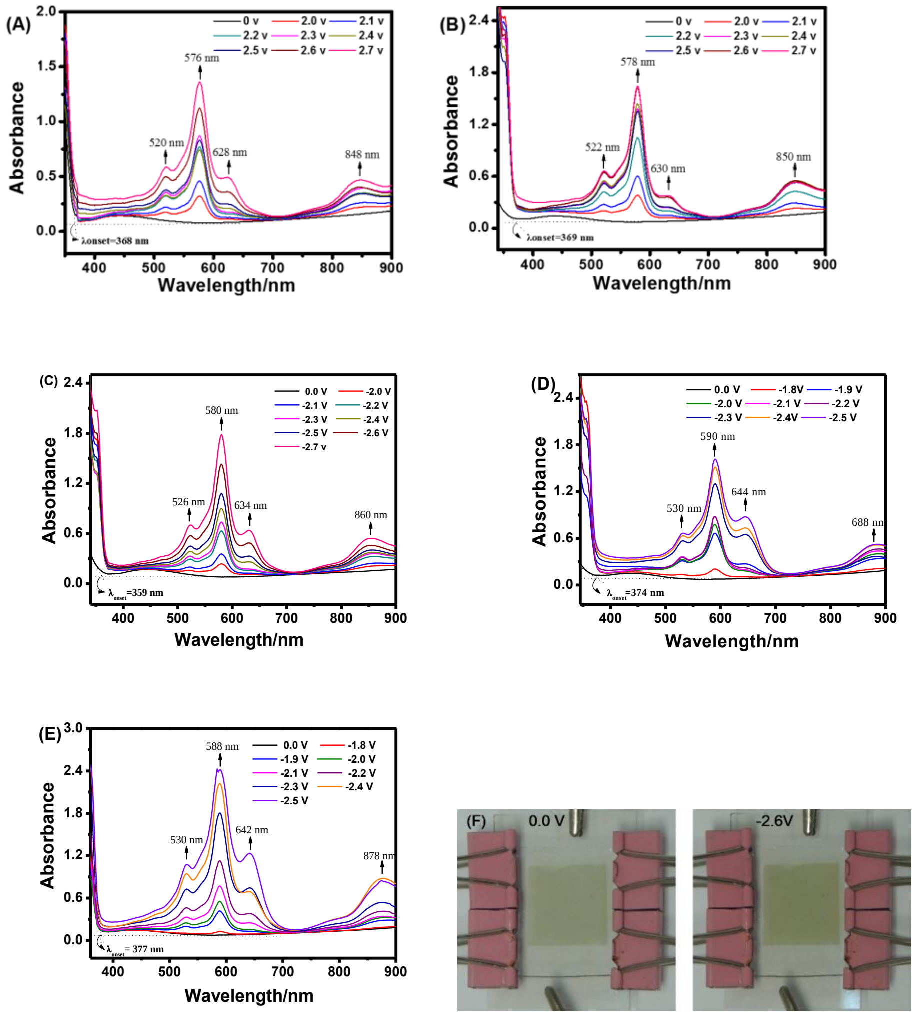

Fig. S12 UV-vis absorption spectra for compound **a** (A), **c** (B), **d** (C), **e** (D), and **g** (E) with a concentration of 20 mmol L^{-1} on indium tin oxide-coated glass at different potentials. (F) Photograph of ECD based on compound **i** upon an applied potential of 0.0 and -2.6 V.

S8 Transmittance change

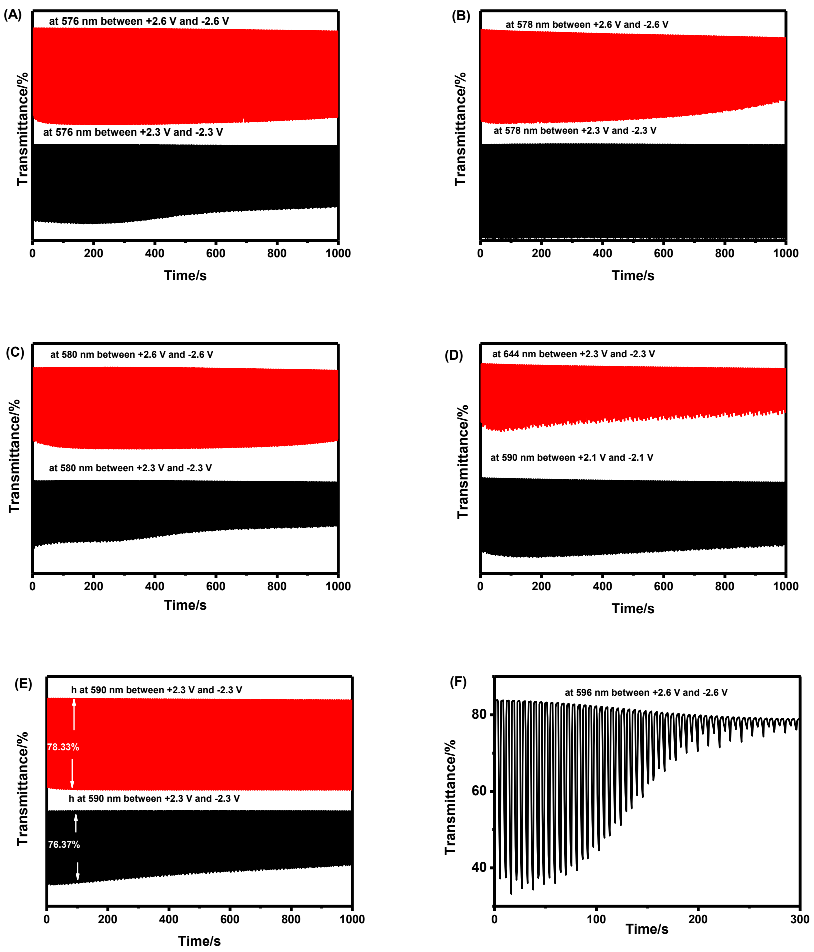

Fig. S13 Transmittance switching stability monitored at the maximum absorption wavelength under the applied potential of ±2.3 V and ±2.6 for compound **b** (A), **c** (B), **d** (C), and ±2.1 V and ±2.3 for compound **e** (D), g (E), and ±2.6 V for compound **h** (F).

S9 Response time

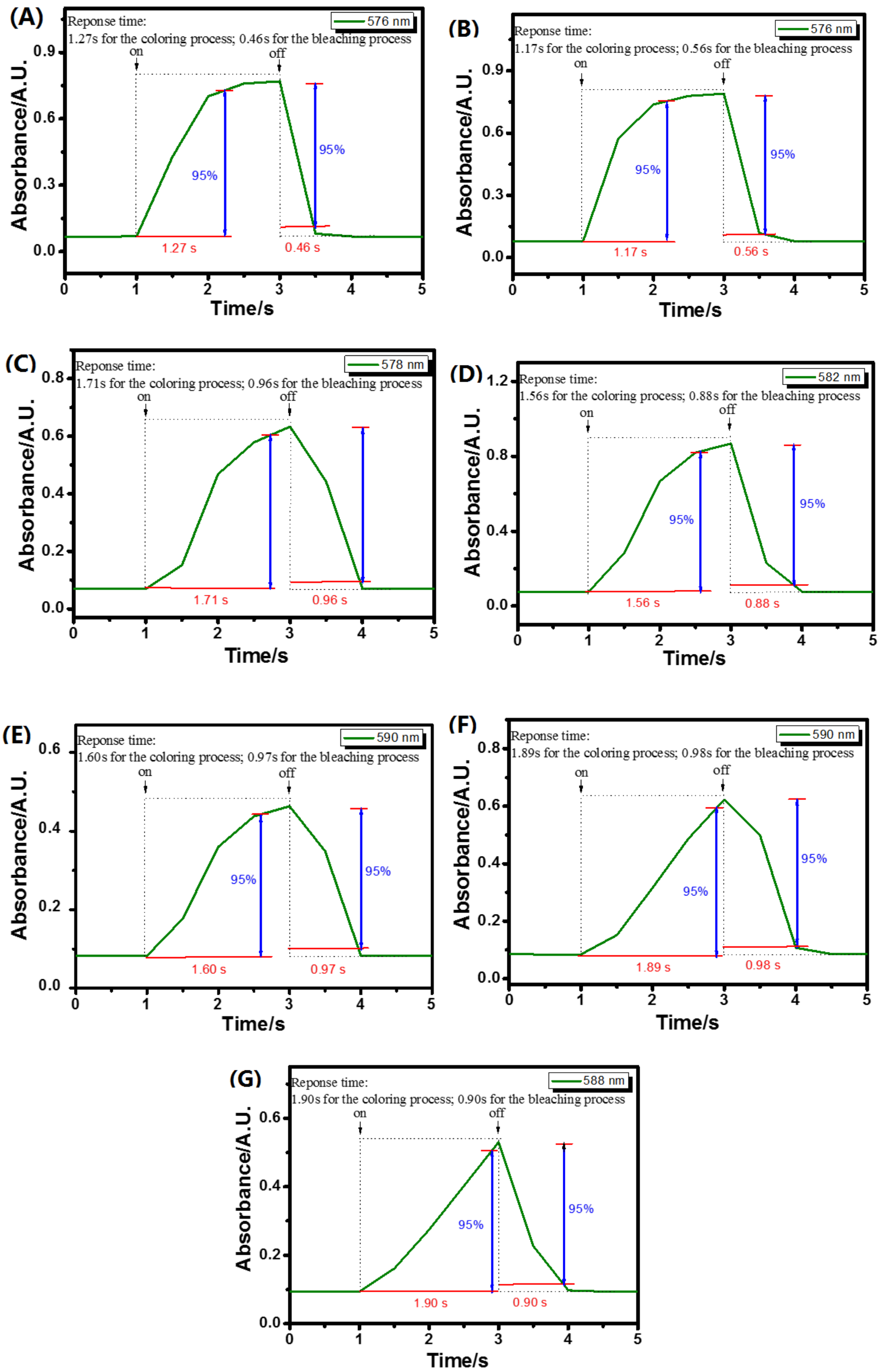

Fig. S14 Optical switching study of ECDs based on compounds **a** (A), **b** (B), **c** (C), **d** (D), **e** (E), **f** (F), and **g** (G) monitored at the maximum absorption wavelength under the applied potential of ±2.3 V for compound **a-d** and ±2.1 V for compound **e-g**.

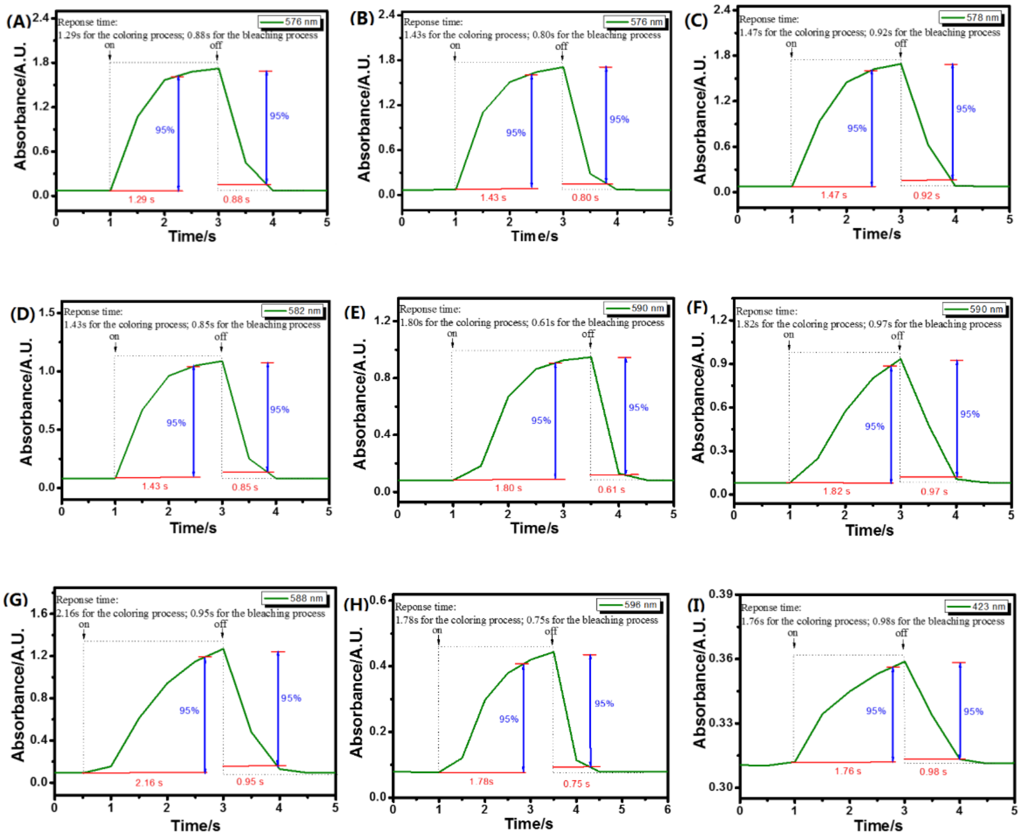

Fig. S15 Optical switching study of ECDs based on compounds **a** (A), **b** (B), **c** (C), **d** (D), **e** (E), **f** (F), **g** (G), **h** (H), and **i** (I) monitored at the maximum absorption wavelength under the applied potential of ±2.6 V for compound **a-d** and ±2.3 V for compound **e-i**.

S10 Coloration efficiency

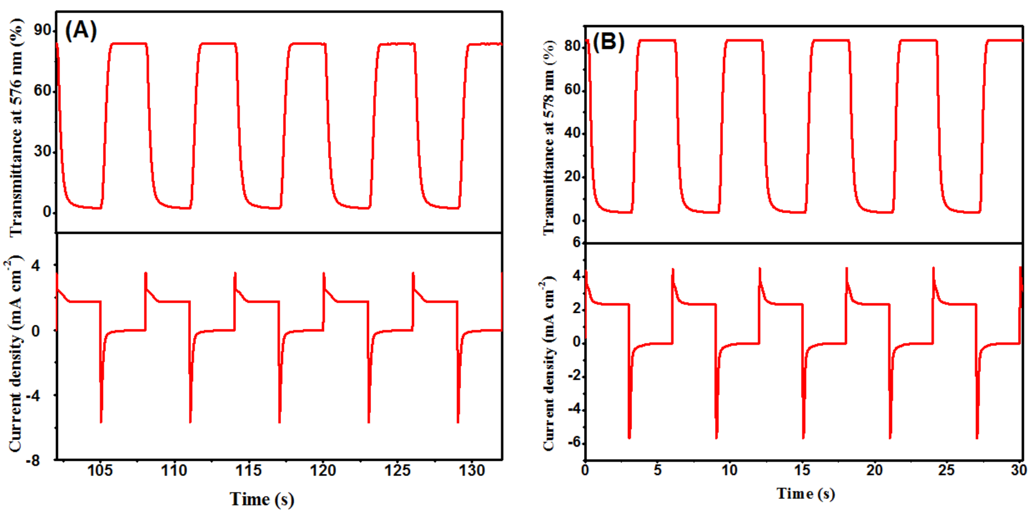

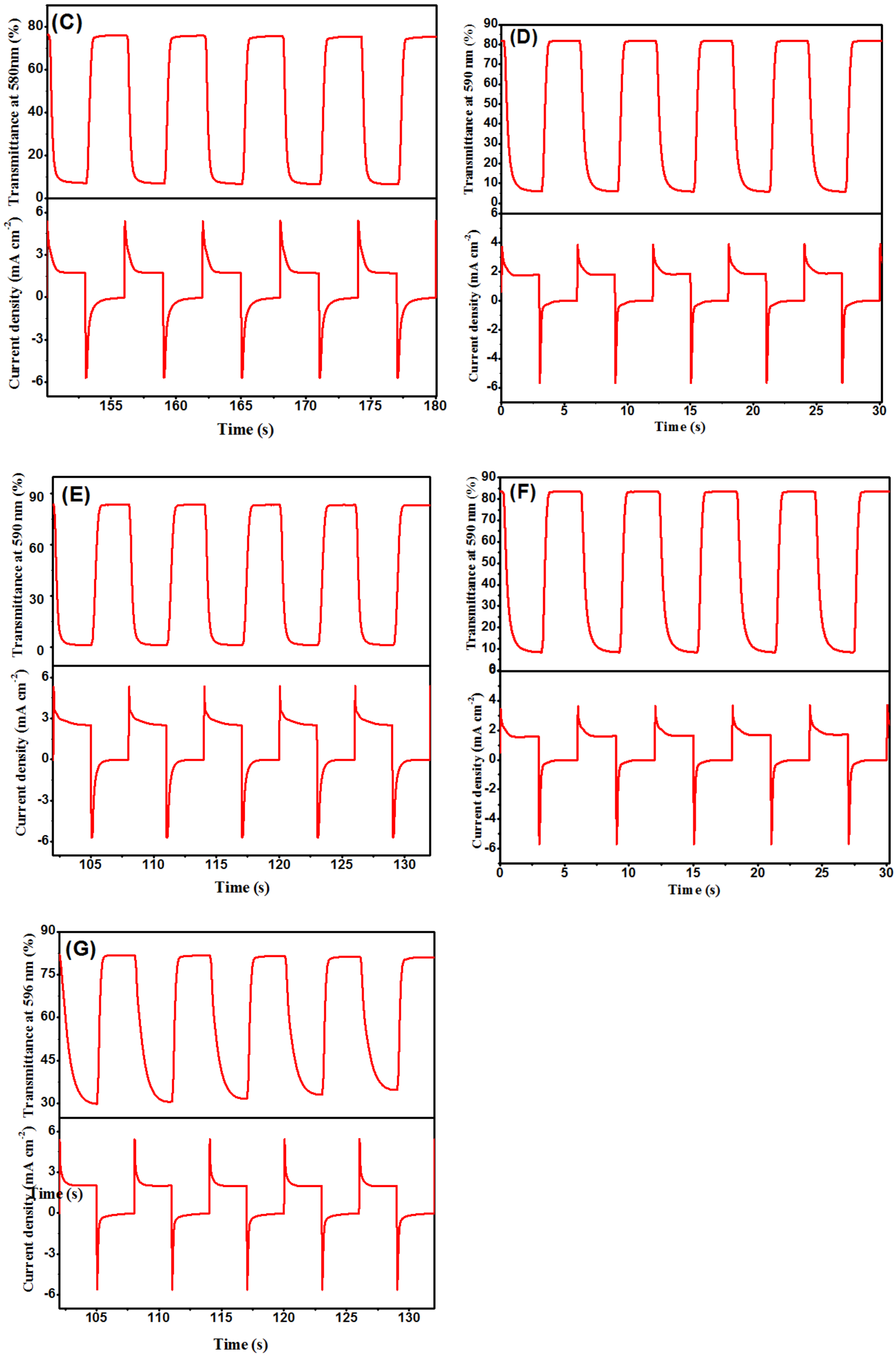

Fig. S16 Chronoamperometry curve and the corresponding in-situ transmittance curve of the ECD based on compounds **b** (A), **c** (B), **d** (C), **e** (D), **f** (E), **g** (F), and **h** (G).

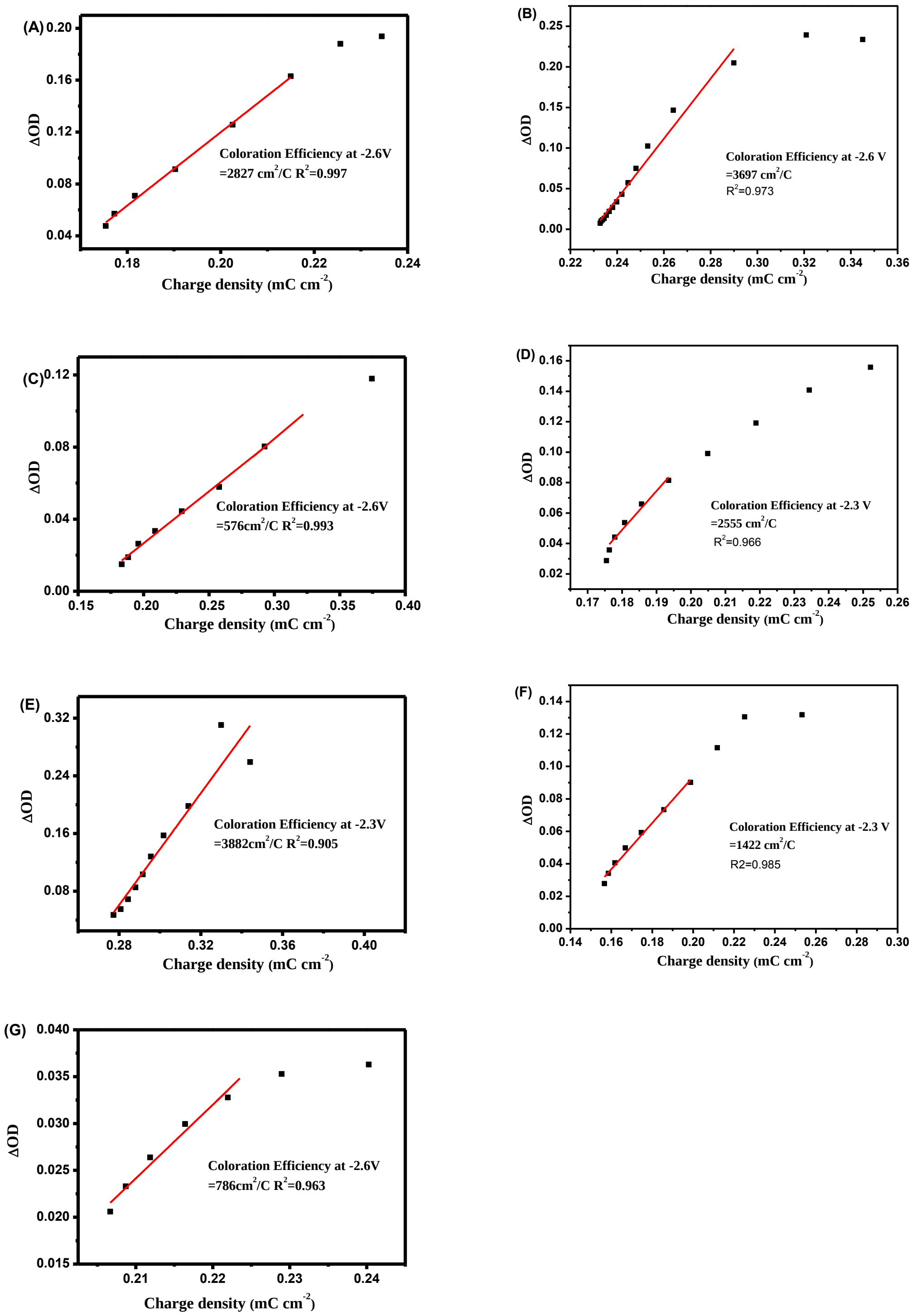

Fig. S17 Optical density versus charge density of the ECD based on compounds **b** (A), **c** (B), **d** (C), **e** (D), **f** (E), **g** (F), and **h** (G).